ELKOMIKA: Jurnal Teknik Energi Elektrik, Teknik Telekomunikasi, & Teknik Elektronika

ISSN(p): 2338-8323 | ISSN(e): 2459-9638 | Vol. 14 | No. 2 | Halaman 261 – 273
DOI : http://dx.doi.org/10.26760/elkomika.v14i2.261 April 2026

Performance Analysis of Inverse Kinematics-Based Balance Control for Hexapod Stair Navigation

Article History:
Received
19 Januari 2026
Revised
12 Februari 2026
Accepted
18 April 2026

SYAFFEL SEAN RIZKINATA HERYAMAN, KHAIRUL ANAM, WAHYU MULDAYANI, ALI RIZAL CHAIDIR, DEDY WAHYU HERDIYANTO, CANDRA PUTRI RIZKIYAH RAMADHANI, AVIQ NURDIANSYAH PUTRA, MUCHAMAD ARIF HANA SASONO

University of Jember, Indonesia
Email: khairul@unej.ac.id

ABSTRAK

Menjaga stabilitas tubuh merupakan tantangan utama bagi robot hexapod dalam navigasi tangga. Penelitian ini mengusulkan pendekatan berbasis inverse kinematics (IK) untuk kendali keseimbangan dinamis melalui perhitungan sudut sendi secara real-time. Hasil eksperimen menunjukkan bahwa metode ini mampu mempertahankan orientasi tubuh mendekati posisi netral dengan pitch minimum 7.3°, sehingga meningkatkan stabilitas dan mengurangi risiko benturan mekanis. Selain itu, performa sistem dipengaruhi oleh kecepatan aktuator dan kestabilan tegangan baterai.

***Kata kunci**: hexapod, inverse kinematics, navigasi tangga, kendali keseimbangan*

ABSTRACT

Maintaining body stability is a key challenge for hexapod robots in stair navigation. This study proposes an inverse kinematics (IK)-based approach for dynamic balance control using real-time joint angle computation. Experimental results show that the method maintains body orientation near a neutral position, achieving a minimum pitch angle of 7.3°, thereby improving stability and reducing mechanical collision risk. System performance is also influenced by actuator speed and battery voltage.

***Keywords**: Hexapod, inverse kinematics, stair navigation, balance control*

1. INTRODUCTION

Hexapod robots, with their six-legged configuration, offer clear advantages in environments where wheeled or tracked robots struggle. Their mechanical design provides high static stability, even load distribution, and redundancy that allows locomotion to continue even if one leg is impaired. These features make hexapods highly suitable for tasks such as search and rescue in collapsed structures, planetary exploration, and inspection of industrial sites **(Coelho, Sa, et al., 2021)(Deng et al., 2017)(Zhang et al., 2024)**. Among several locomotion challenges, stair climbing represents one of the most demanding scenarios. It requires the precise coordination between multiple legs, The accurate foot placement on discrete step edges, and continuous regulation of body posture. The sudden changes in elevation introduced by stairs amplify the effects of actuation errors and sensor inaccuracies, often leading to loss of balance or failed traversal if not carefully managed **(Coelho et al., 2021)(Konopatzki et al., 2022)**.

Previous research in legged locomotion has advanced substantially in gait generation, stability analysis, and trajectory planning, with most studies centered on flat or mildly uneven terrain. Approaches such as central pattern generators (CPGs), stability margin optimization, and inverse kinematics (IK) have been widely used in simulation studies and have provided a strong theoretical basis for efficient legged motion **(Garcia & de Santos, 2005)(Saranli et al., 2001)(Zhang et al., 2023)**. Within this context, several works have demonstrated the promise of IK-based methods for stair climbing, primarily through simulation experiments that highlight their ability to manage discrete step transitions **(Sun et al., 2018)(Wang et al., 2020)**.

However, systematic experimental validation remains limited, particularly for hexapod robots. Most empirical studies on stair negotiation have been conducted with quadrupeds and humanoids, where researchers examined joint trajectories, balance strategies, and sensor performance under controlled conditions **(Xu et al., 2023)(Zhang et al., 2017)**. These works have established valuable insights, but they cannot be directly generalized to hexapods, which rely on distinct stability mechanisms and leg redundancy. For hexapods specifically, comprehensive datasets from real stair environments remain scarce **(Ramdya et al., 2017)**. Without such data, it is difficult to assess whether theoretical IK models can reliably support locomotion on complex terrains beyond simulation.

To address this gap, more rigorous experimental studies are needed that examine not only joint configurations but also actuator conditions and sensor feedback during stair negotiation. Biological studies of insect locomotion suggest that distributed sensing and adaptive gait modulation are key for stability on irregular terrain **(Fielding & Dunlop, 2004)(Zhu et al., 2017)**. Integrating these biologically inspired principles into IK-based approaches could enhance robustness, but such integration must be grounded in empirical trials with physical hexapod platforms **(Xia et al., 2021)**.

2. METHOD

2.1 Mechanical Design of the Hexapod Platform

The hexapod robot was designed with a compact, modular body that ensures high structural stability while maintaining a lightweight configuration suitable for experimental stair navigation. The robot measures 25 cm in length, 22.5 cm in width, and 22.15 cm in height, achieving a low center of gravity essential for maintaining balance during discrete step transitions. The chassis and leg brackets are fabricated from 5 mm acrylic plates for the base

structure and 3 mm panels for the upper housing, providing sufficient rigidity while keeping the total mass around 2.7 kg

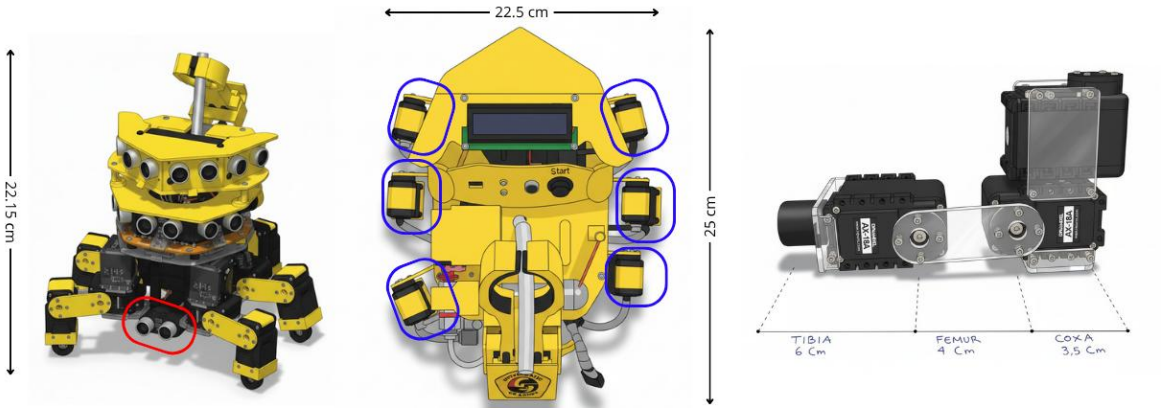

(a) **(b)** **(c)**

Figure 1. Mechanical structure and leg geometry of the developed hexapod robot. (a) Isometric 3D view showing the overall leg configuration, six-leg symmetry, and front-mounted ultrasonic sensor for stair detection; (b) Top view with servo placement highlighted in blue and the overall body dimensions indicated; (c) Single-leg geometry illustrating the 3-DOF chain

Each of the six identical legs possesses three degrees of freedom (3-DOF) driven by Dynamixel AX-18A smart servomotors, resulting in a total of 18 actuators across the robot. The joints correspond to the coxa, femur, and tibia segments, configured in a serial 3R chain that enables precise motion in the sagittal and vertical planes. The segment lengths were determined through empirical optimization to balance step height capability and mechanical leverage. This geometry allows the robot to achieve a stride length of approximately 12 cm while maintaining sufficient torque margin on each joint for climbing 6 cm stairs.

A PING ultrasonic sensor is mounted on the lower-front section of the robot to detect stair edges, while a CMPS14 IMU assists in maintaining body orientation. For inverse-kinematics calculations, each leg follows a 3R kinematic chain with measured link lengths of Coxa 3.5 cm, Femur 4 cm, and Tibia 6 cm, forming the fundamental geometric basis for trajectory generation during ascent and descent.

2.2 Hardware Architecture

The hexapod employs a dual-controller hardware architecture designed to separate high-level computation from actuator control. An Arduino Due functions as the main processing unit, acquiring data from the CMPS14 IMU via I²C and the PING ultrasonic sensor via digital input. This controller performs stair detection and inverse-kinematics computation before sending movement commands to the secondary controller. Actuator control is handled by OpenCM 9.04, which drives all 18 Dynamixel AX-18A servomotors through a TTL half-duplex bus. The servos are assigned IDs 1–18 and grouped into front, mid, and rear legs to streamline motion sequencing during stair traversal.

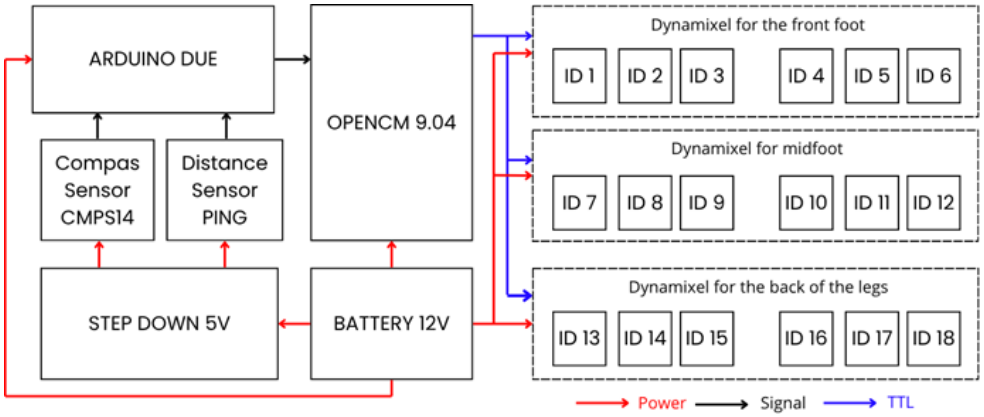

Figure 2. Hardware architecture of the hexapod showing the dual-controller system, sensor interfaces, and Dynamixel actuator network

A 12 V battery supplies power directly to all servos and the OpenCM module, while a 5 V step-down regulator provides stable power for both sensors. This distribution minimizes voltage drops during high-torque movements and ensures consistent signal integrity across the system.

2.3 Inverse-kinematic Formulation

The inverse-kinematics (IK) formulation establishes the mathematical relationship between a desired foot position (x, y, z) and the corresponding joint angles of the coxa, femur, and tibia. The model follows the physical leg geometry of the hexapod, which is structured as a 3R serial manipulator operating in the sagittal plane, combined with a horizontal rotational degree of freedom at the coxa. The geometric parameters used in this formulation are illustrated in Figure 3.

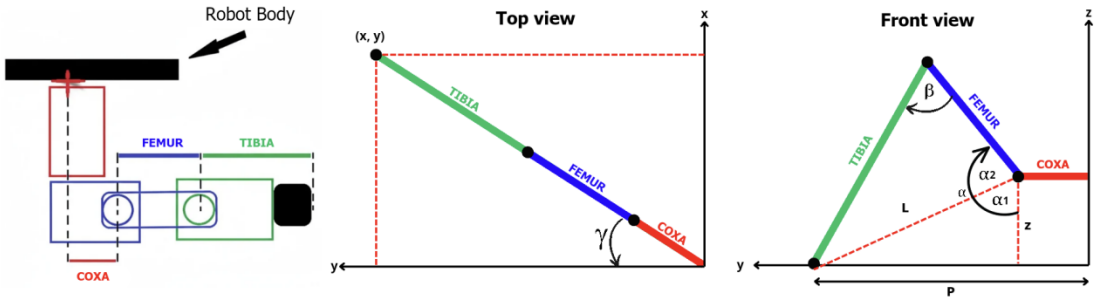

Figure 3. (a) Linkage representation of the coxa–femur–tibia joints; (b) Top-view projection showing the computation of the coxa angle γ; (c) Sagittal-plane kinematic model used to derive femur and tibia angles α and β through geometric relationships

Figure 3(a) depicts the physical arrangement of the three link segments together with their rotational axes. The body pitch of the robot is considered relative to the horizontal plane, where $0°$denotes level ground, positive inclination represents stair ascent, and negative inclination corresponds to descent. Variations in body pitch directly influence the vertical target coordinate z, thereby affecting the required femur-tibia configuration. In Figure 3(b), the desired foothold (x, y) is projected onto the horizontal plane, allowing the coxa joint to align the leg toward the target through a single rotational motion. This reduces the remaining IK problem to a planar 2-link chain. Figure 3(c) provides the sagittal-plane geometry used to derive the femur and tibia angles, where the horizontal projection $P$and effective reach L

define the triangle formed by the femur–tibia linkage. The inverse-kinematics formulation of the hexapod leg is derived from the geometric relationship between the desired foot position (x, y, z) and the three actuated joints: coxa, femur, and tibia. The computation begins by projecting the target position onto the horizontal plane to obtain the ground-referenced distance. To compute the joint angles, the target position is first projected onto the ground plane

$$P = \sqrt{x^2 + y^2} \tag{1}$$

The coxa joint rotates to face the target position via:

$$\gamma = tan^{-1}\left(\frac{x}{y}\right) \tag{2}$$

ensuring that the remaining joints operate in a single plane. After compensating for the physical coxa length, the effective distance from the femur joint to the foot is obtained as

$$L = \sqrt{(P - coxa)^2 + z^2} \tag{3}$$

which is used to resolve the femur–tibia triangle. Applying the cosine law yields the tibia angle:

$$\beta = cos^{-1}\left(\frac{tibia^2 + femur^2 - L^2}{2 \times\ tibia \times femur}\right) \tag{4}$$

while the femur angle is obtained by summing two components. The first term captures the elevation angle needed to reach the vertical component of the foothold

$$\alpha_1 = cos^{-1}\left(\frac{z}{L}\right) \tag{5}$$

and the second describes the internal geometric constraint between the femur and tibia

$$\alpha_2 = cos^{-1}\left(\frac{femur^2 + L^2 - tibia^2}{2\ \times\ femur\ \times L}\right) \tag{6}$$

Thus, the overall femur angle used for actuation is

$$\alpha = \alpha_1 + \alpha_2 \tag{7}$$

Together, these equations specify the complete joint-space solution for each leg. The parameter γdetermines horizontal leg orientation, αgenerates the required lifting and forward reach during climbing motion, and βgoverns extension during the support and swing phases. Although identical in formulation, the target coordinates (x, y, z)vary across front, middle, and rear legs to accommodate the geometric constraints encountered during flat walking, stair ascent, and stair descent.

2.4 Body-Pitch Characterization for Stair Navigation

Before evaluating full locomotion, the robot's body orientation was characterized to determine the pitch ranges that yield optimal static stability during stair climbing and descending. Using the CMPS14 sensor, pitch measurements were collected on flat ground, a standard stair riser,

and inclined transition surfaces. The robot exhibited a nominal flat-ground reference of $0°$, with stable ascending configurations occurring near $+20°$to $+25°$, and stable descending configurations appearing in the range of $315°–335°$ (equivalent to $-25°$to $-45°$). These values were essential for two reasons. First, they served as closed-loop setpoints for the pitch stabilization controller used during stair traversal. Second, they provided the reference vertical shift applied to the IK target coordinate $\boldsymbol{z}$, ensuring each leg trajectory remained consistent with the true geometric posture of the robot. By linking body inclination to the inverse-kinematic solution, the method prevented overextension or premature ground contact—two common failure modes in hexapod stair navigation.

2.5 Leg-Trajectory Structuring for Ascent and Descent

Because each leg segment interacts with the stairs differently, the foot trajectories were individually parameterized for the front, middle, and rear legs, while still using the same IK equations defined in sub section C. Front legs were assigned elevated swing trajectories to ensure clearance of the stair edge.

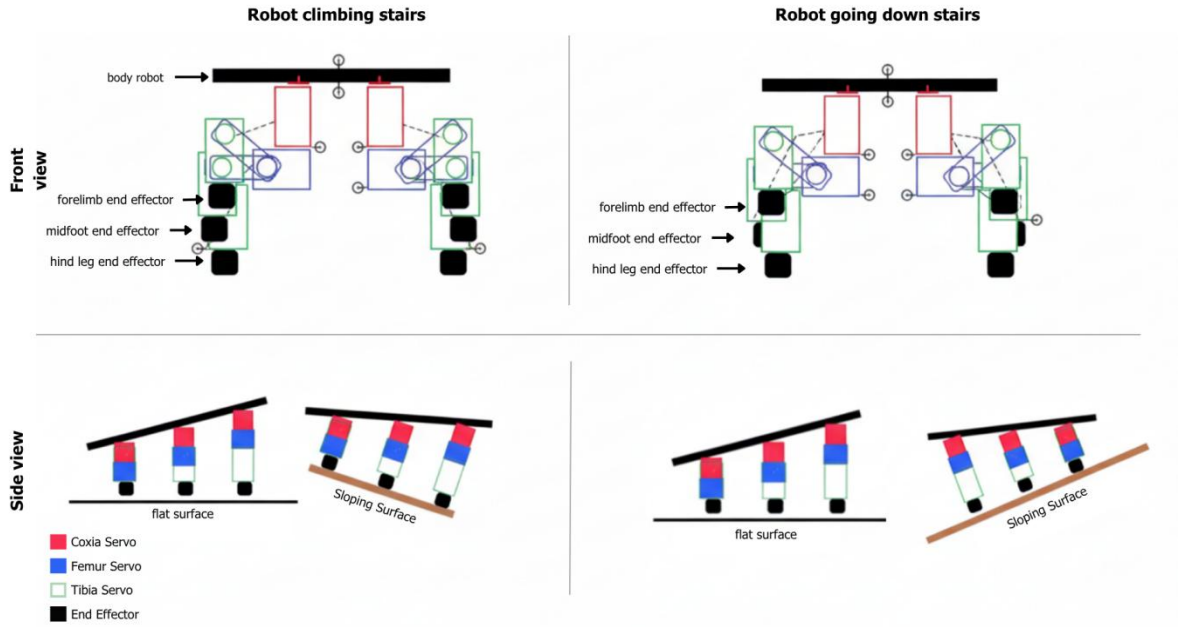

Figure 4. Leg-trajectory configurations during stair ascent (left) and descent (right), shown from front and side views for forelimb, midfoot, and hind-leg end-effectors.

Their target height z was increased relative to flat-ground walking, with a forward offset in x to place the foot onto the next riser. Middle legs acted as stabilizers, maintaining a trajectory closer to the body to stabilize the center of mass during the lifting phase. These legs provided the majority of load bearing during the transition between risers. Rear legs were assigned a downward offset during ascent so that they could push the body upward from a lower riser. During descent, their trajectories were raised earlier to prevent foot entrapment against the upper step surface

3. RESULTS AND DISCUSSION

3.1 Sensor Performance

Preliminary experiments were conducted to ensure that the sensor and communication systems were capable of providing reliable data as a basis for inverse kinematics control. The

evaluation focused on the accuracy of the PING ultrasonic sensor in detecting stair distance and the precision of the CMPS14 sensor in measuring the roll and pitch orientation of the robot body.

Table 1. Summary of PING Ultrasonic Sensor and CMPS14 Performance

Test Parameter	Test Range	Avg Error	Description
PING Ultrasonic Sensor (Distance)	0.5 – 60 cm	19.04%	Error mainly occurs at extreme distances; accurate within the operational range
CMPS14 Roll Angle	0° – 330°	0.58°	Stable and consistent readings
CMPS14 Pitch Angle	0° – 330°	0.14°	Very stable readings

The results of the PING sensor tests indicate that distance measurements are accurate within the main operational range of the system, particularly from distances greater than or equal to 2 cm up to 40 cm, where the measurement error is close to zero. Significant errors were observed only at very short distances (≤ 1 cm) and at extended distances above 50 cm, which are outside the operational requirements for stair edge detection. Overall, the PING sensor is considered adequate for triggering stair ascent and descent modes. Testing of the CMPS14 sensor shows very small angular deviations for both roll and pitch measurements. The average deviation for roll is 0.58°, while the pitch deviation is 0.14°. These results indicate that the sensor provides stable and consistent body orientation estimates, making it sufficiently precise to be used as feedback for balance control during stair climbing and descending.

3.2 Inverse Kinematics Performance During Stair Ascent

To evaluate the effect of inverse kinematics on body stability during stair ascent, several leg position configurations were tested. Each configuration was assessed based on the resulting body pitch angle, which represents the overall stability of the robot while climbing the stairs.

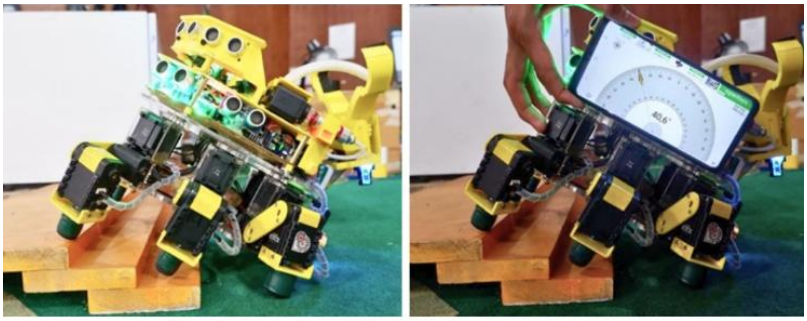

(a) **(b)**

Figure 5. (a) Actual body tilt of the robot during stair ascent, (b) Measurement of the robot body tilt angle during stair ascent

Table 2 summarizes the inverse kinematics results for stair ascent under different leg position configurations. Each test represents a different combination of foot positions for the front, middle, and rear legs, and the resulting body pitch angle is used as an indicator of stability. The results show that lower body pitch values correspond to more stable climbing conditions. Among the tested configurations, the first test produced the smallest body pitch angle.

Table 2. Inverse Kinematics Results During Stair Ascent

Test	Leg	Input (X,Y,Z) cm	Joint Angles (γ, α, β) °	Body Pitch (°)
1	Front	(5,5,3)	(45, 137.27, 50.94)	**7.36**
	Middle	(5,5,5)	(45, 104.36, 72.73)	
	Rear	(5,5,7)	(45, 75.41, 101.72)	
2	Front	(5,5,3.5)	(45, 128.39, 55.77)	**14.00**
	Middle	(5,5,4)	(45, 119.98, 61.03)	
	Rear	(5,5,6)	(45, 89.78, 86.12)	
3	Front	(5,5,5)	(45, 104.36, 72.73)	**25.42**
	Middle	(5,5,5)	(45, 104.36, 72.73)	
	Rear	(5,5,5)	(45, 104.36, 72.73)	
4	Front	(5,5,5)	(45, 104.36, 72.73)	**31.29**
	Middle	(5,5,4)	(45, 119.98, 60.03)	
	Rear	(5,5,3.5)	(45, 128.39, 55.77)	
5	Front	(5,5,7)	(45, 75.41, 101.72)	**43.30**
	Middle	(5,5,5)	(45, 104.36, 72.73)	
	Rear	(5,5,3)	(45, 137.27, 50.94)	

indicating the most stable posture during stair ascent, while larger pitch angles in subsequent tests reflect reduced stability as the leg configuration changes.

3.3 Inverse Kinematics Performance During Stair Descent

To analyze the effect of inverse kinematics on robot stability, several leg position configurations were tested during stair traversal. The body pitch angle was used as the main indicator to evaluate the stability of each configuration. Table 3 shows that different leg position configurations result in varying body pitch angles. Lower pitch values indicate more stable robot posture, while higher pitch values reflect reduced stability. The first configuration produces the smallest pitch angle and represents the most stable condition, whereas later configurations lead to a significant increase in body inclination.

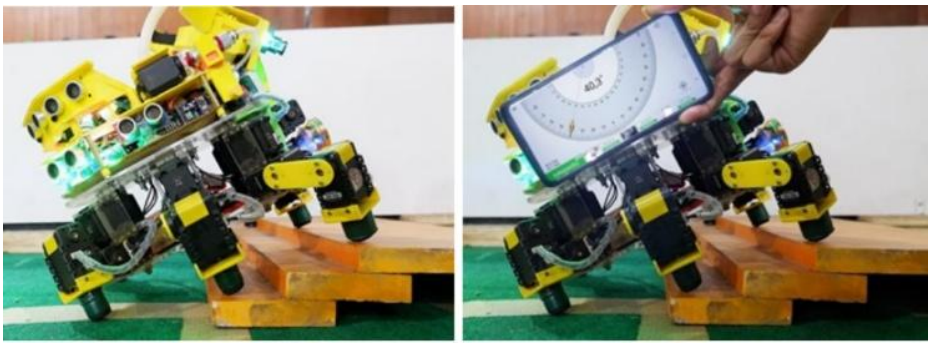

(a) **(b)**

Figure 6. (a) Actual robot body tilt during stair descent, (b) Measurement of robot body tilt angle during stair descent

Table 3. Inverse Kinematics Results During Stair Descent

Test	Leg	Input (X,Y,Z) cm	Joint Angles (γ, α, β) °	Body Pitch (°)
1	Front	(5,5,7)	(45, 75.41, 101.72)	**7.36**
	Middle	(5,5,5)	(45, 104.36, 72.73)	
	Rear	(5,5,3)	(45, 137.27, 50.94)	
2	Front	(5,5,6)	(45, 89.78, 86.12)	**14.00**
	Middle	(5,5,4)	(45, 119.98, 61.03)	
	Rear	(5,5,3.5)	(45, 128.39, 55.77)	
3	Front	(5,5,5)	(45, 104.36, 72.73)	**25.42**
	Middle	(5,5,5)	(45, 104.36, 72.73)	
	Rear	(5,5,5)	(45, 104.36, 72.73)	
4	Front	(5,5,3.5)	(45, 128.39, 55.77)	**31.29**
	Middle	(5,5,4)	(45, 119.98, 61.03)	
	Rear	(5,5,5)	(45, 104.36, 72.73)	
5	Front	(5,5,7)	(45, 75.41, 101.72)	**43.30**
	Middle	(5,5,5)	(45, 104.36, 72.73)	
	Rear	(5,5,3)	(45, 137.27, 50.44)	

The figure shows the hexapod robot during stair descent. The robot maintains a stable body posture while stepping down, and the body tilt angle is monitored to ensure balance during the descent process.

3.4 Overall System Evaluation and Discussion

To evaluate the overall performance of the robot, a series of stair-climbing tests were conducted under different actuator speed and battery voltage conditions. The success rate and traversal time were recorded to observe the effect of these parameters on stair-climbing reliability. Table 4 demonstrates that traversal time is not merely an auxiliary metric, but a key indicator of overall stair-climbing performance. A consistent trend is observed in which increasing PWM values reduces traversal time while simultaneously improving traversal reliability. At a battery voltage of 12.60 V, the traversal time decreases from 30 s at PWM 133 to 28 s at PWM 160, 22 s at PWM 200, and 19 s at PWM 250, indicating a clear improvement in locomotion efficiency with higher actuator speed. In contrast, at PWM 133, a reduction in battery voltage from 12.60 V to 12.45 V increases traversal time from 30 s to 35 s, and further voltage drops to 12.25 V and 12.00 V result in traversal failure due to insufficient step clearance, causing the feet to become stuck on the stair edge.

Table 4. Overall Stair-Climbing Test Results

Test	Success	Time (s)	PWM (Max)	Battery (V)	Remarks
1	Yes	30	133	12.60	Stable traversal
2	Yes	35	133	12.45	Stable traversal
3	No	37	133	12.25	Low speed, foot stuck on stair
4	No	38	133	12.00	Low speed, foot stuck on stair
5	Yes	28	160	12.60	Stable traversal
6	Yes	30	160	12.50	Stable traversal
7	Yes	22	200	12.60	Faster traversal
8	Yes	25	200	12.50	Faster traversal
9	Yes	19	250	12.60	Fastest traversal
10	Yes	22	250	12.50	Stable traversal

These results indicate that overall performance is strongly influenced by the interaction between control strategy and hardware conditions. While the inverse kinematics (IK) controller ensures coordinated joint motion and stable posture, successful stair traversal depends critically on sufficient actuator speed and a stable power supply to maintain forward momentum and adequate foot clearance. In particular, low PWM conditions make the system more sensitive to voltage fluctuations, leading to reduced reliability. Therefore, traversal time reflects not only motion efficiency but also the system's ability to sustain stable locomotion under practical operating constraints. However, given the limited number of trials and the absence of a fully factorial evaluation of PWM and voltage, these findings should be interpreted as indicative trends rather than definitive causal relationships.

3.5 Comparison with Non-Inverse Kinematics Approaches

A comparison with prior non-inverse-kinematics (non-IK) approaches indicates that stable stair and slope traversal can also be achieved through alternative control strategies, including open-loop compliant-leg control, central pattern generator (CPG)-based gait generation, adaptive gait-parameter adjustment, and posture-control frameworks, as shown in Table 5. For example, Moore et al. reported climbing and descending reliabilities of 90% and 100%, respectively, on full-scale stairs using an open-loop controller on the RHex platform **(Moore et al., n.d.)**. Wang et al. demonstrated that a feedback Hopf-based gait reduced body pitch during 16° slope climbing from approximately 14.5°–16.5° to 5.5°–7.5°, highlighting the importance of posture regulation **(Wang et al., 2020)**. In addition, Zhao et al. achieved autonomous traversal of multiple stair steps with rapid gait adaptation (≈100 ms update time) **(Zhao et al., 2020)**, while Liu et al. reported a maximum pitch of approximately 11° during stepped-terrain locomotion using a posture-control strategy **(Liu et al., 2020)**.

Compared with these approaches, the proposed inverse-kinematics-based method achieves a minimum body pitch of 7.36° during both ascent and descent, demonstrating competitive performance in maintaining body stability. More importantly, the IK formulation provides an explicit and deterministic joint-space solution for coordinating the front, middle, and rear legs, which simplifies trajectory control in discrete stair environments. Nevertheless, direct quantitative comparison should be interpreted with caution, as differences in robot morphology, terrain geometry, and evaluation protocols may significantly influence the reported performance.

Table 5. Comparison between IK-based and non-IK-based stair locomotion methods

Study	Control Strategy	IK Usage	Test Scenario	Key Quantitative Result	Stability Indicator
(Moore et al., n.d.)	Open-loop compliant-leg control	No	Full-scale stairs	Climbing: 90%, Descending: 100% success rate	-
(Wang et al., 2020)	CPG (Hopf oscillator) with feedback	No	16° slope climbing	Pitch reduced from 14.5°–16.5° to 5.5°–7.5°	Body pitch
(Zhao et al., 2020)	Adaptive gait-parameter adjustment	No	Multi-step stairs (130 × 300 mm)	Gait update time ≈ 100 ms	-
(Liu et al., 2020)	Posture-control framework	No	Stepped terrain	Max pitch ≈ 11°	Body pitch
This study	**Inverse kinematics-based control**	**Yes**	Stair ascent & descent	Min pitch: **7.36°**	Body pitch

4. CONCLUSION

This study demonstrates that the empirical implementation of inverse kinematics (IK) can effectively support stable stair navigation in a hexapod robot by enabling coordinated joint control and maintaining the body pitch within a relatively low range, with a minimum value of 7.36°. A comparison with non-IK-based approaches indicates that stable locomotion can also be achieved through gait adaptation and posture-control strategies; however, the proposed IK method provides a more explicit and structured joint-space formulation for stair-specific motion. Furthermore, the time-test analysis shows that overall performance is influenced not only by the control strategy but also by hardware conditions, where higher actuator speeds reduce traversal time and improve reliability, while low PWM combined with reduced battery voltage leads to increased traversal time and potential failure due to insufficient foot clearance. These findings highlight that robust stair-climbing performance arises from the interaction between kinematic control and hardware capability, suggesting that both aspects must be jointly considered in practical hexapod locomotion systems.

REFERENCES

Coelho, J., Ribeiro, F., Dias, B., Lopes, G., & Flores, P. (2021). Trends in the Control of Hexapod Robots: A Survey. *Robotics*, *10*(3), 100. https://doi.org/10.3390/robotics10030100

Coelho, J., Sa, R., Ribeiro, T., Ribeiro, F., Dias, B., Lopes, G., & Flores, P. (2021). Study of the locomotion of a hexapod using CoppeliaSim and ROS. *2021 International Conference on Computers and Automation (CompAuto)*, (pp. 109–116). https://doi.org/10.1109/CompAuto54408.2021.00027

Deng, H., Xin, G., Zhong, G., & Mistry, M. (2017). Gait and trajectory rolling planning and control of hexapod robots for disaster rescue applications. *Robotics and Autonomous Systems*, *95*, 13–24. https://doi.org/10.1016/j.robot.2017.05.007

Fielding, M. R., & Dunlop, G. R. (2004). Omnidirectional Hexapod Walking and Efficient Gaits Using Restrictedness. *The International Journal of Robotics Research*, *23*(10–11), 1105–1110. https://doi.org/10.1177/0278364904047396

Garcia, E., & de Santos, P. G. (2005). An improved energy stability margin for walking machines subject to dynamic effects. *Robotica*, *23*(1), 13–20. https://doi.org/10.1017/S0263574704000487

Konopatzki, E. A., Christ, D., Coelho, S. R. M., Demito, A., Werncke, I., & Camicia, R. G. da M. (2022). COFFEE DRYER WITH DEHYDRATED AIR: A TECHNICAL AND ECONOMIC VIABILITY ANALYSIS. *Engenharia Agrícola*, *42*(4). https://doi.org/10.1590/1809-4430-eng.agric.v42n4e20210003/2022

Liu, Y., Wang, C., Zhang, H., & Zhao, J. (2020). Research on the Posture Control Method of Hexapod Robot for Rugged Terrain. *Applied Sciences*, *10*(19), 6725. https://doi.org/10.3390/app10196725

Moore, E. Z., Campbell, D., Grimminger, F., & Buehler, M. (n.d.). Reliable stair climbing in the simple hexapod "RHex." *Proceedings 2002 IEEE International Conference on Robotics and Automation (Cat. No.02CH37292)*, *3*, 2222–2227. https://doi.org/10.1109/ROBOT.2002.1013562

Ramdya, P., Thandiackal, R., Cherney, R., Asselborn, T., Benton, R., Ijspeert, A. J., & Floreano, D. (2017). Climbing favours the tripod gait over alternative faster insect gaits. *Nature Communications*, *8*(1), 14494. https://doi.org/10.1038/ncomms14494

Saranli, U., Buehler, M., & Koditschek, D. E. (2001). RHex: A Simple and Highly Mobile Hexapod Robot. *The International Journal of Robotics Research*, *20*(7), 616–631. https://doi.org/10.1177/02783640122067570

Sun, Q., Gao, F., & Chen, X. (2018). Towards dynamic alternating tripod trotting of a pony-sized hexapod robot for disaster rescuing based on multi-modal impedance control. *Robotica*, *36*(7), 1048–1076. https://doi.org/10.1017/S026357471800022X

Wang, B., Zhang, K., Yang, X., & Cui, X. (2020). The gait planning of hexapod robot based on CPG with feedback. *International Journal of Advanced Robotic Systems*, *17*(3). https://doi.org/10.1177/1729881420930503

Xia, H., Zhang, X., & Zhang, H. (2021). A New Foot Trajectory Planning Method for Legged Robots and Its Application in Hexapod Robots. *Applied Sciences*, *11*(19), 9217. https://doi.org/10.3390/app11199217

Xu, P., Ding, L., Li, Z., Yang, H., Wang, Z., Gao, H., Zhou, R., Su, Y., Deng, Z., & Huang, Y. (2023). Learning physical characteristics like animals for legged robots. *National Science Review*, *10*(5). https://doi.org/10.1093/nsr/nwad045

Zhang, H., Wu, R., Li, C., Zang, X., Zhang, X., Jin, H., & Zhao, J. (2017). A Force-Sensing System on Legs for Biomimetic Hexapod Robots Interacting with Unstructured Terrain. *Sensors*, *17*(7), 1514. https://doi.org/10.3390/s17071514

Zhang, L., Zha, F., Guo, W., Chen, C., Sun, L., & Wang, P. (2024). Heavy-duty hexapod robot sideline tipping judgment and recovery. *Robotica*, *42*(5), 1403–1419. https://doi.org/10.1017/S0263574724000274

Zhang, Y., Qiao, G., Wan, Q., Tian, L., & Liu, D. (2023). A Novel Double-Layered Central Pattern Generator-Based Motion Controller for the Hexapod Robot. *Mathematics*, *11*(3), 617. https://doi.org/10.3390/math11030617

Zhao, Y., Gao, F., Tian, Y., & Mao, L. (2020, August 24). Adaptive gait parameters adjustment strategy for a hexapod robot walking on stairs based on 3D terrain perception. *Robots in Human Life*. https://doi.org/10.13180/clawar.2020.24-26.08.09

Zhu, Y., Guo, T., Liu, Q., Zhu, Q., Jin, B., & Zhao, X. (2017). Turning and Radius Deviation Correction for a Hexapod Walking Robot Based on an Ant-Inspired Sensory Strategy. *Sensors*, *17*(12), 2710. https://doi.org/10.3390/s17122710